Method for visualizing volumetric caustics in single-scattering media based on beam tracking

Olexandr Romanyuk[*a], Hamza Achanyar[b], Roman Chekhmestruk[c], Pavlo Mykhaylov[d], Nataliia Savina[e], Iryna Shvarts[a], Volodymyr Kistion[f], Zbigniew Omiotek[g], Nurbapa Mekebayev[h]
[a]Vinnytsia National Technical University, Vinnytsia, Ukraine; [b]DRESSLAB GmbH, Dortmund, Germany; [c]3D GENERATION UA, Vinnitsa, Ukraine; [d]CEO 3D GNERATION GmbH, Dortmund, Germany; [e]National University of Water and Environmental Engineering, Rivne, Ukraine; [f]Kyiv National University of Construction and Architecture, Kyiv, Ukraine; [g]Lublin University of Technology, Lublin, Poland; [h]Al-Farabi Kazakh National University, Almaty, Kazakhstan

ABSTRACT

A method of visualization of surface and volumetric caustics of reflected and refracted light on mirror surfaces in volume and on functionally specified surfaces consisting of patches of free forms is proposed. Caustics are surfaces near which the intensity of the light field increases sharply. The visualization method tracks the rays of light in the light space when displaying mirror surfaces. Light rays are projected from light sources onto patches of free-form scenes. The limiting volumes of caustic rays are determined, thereby reducing the number of calculations. Only caustic rays are calculated, which make the main contribution to the resulting image.

Keywords: surface caustics, volumetric caustics, beam tracing, free-form patch, perturbation functions

1. INTRODUCTION

Caustics is the envelope of a family of rays that do not converge at one point. Caustics appear not only in the propagation of light, but also in many other wave phenomena. In optics, caustics are lines (in the two-dimensional case) and surfaces of infinitesimal thickness. Caustics are the evolute of the wave front, and the wave front is the involute of caustics. Caustics have a small thickness, but not less than the wavelength of light. It depends on the wave properties of the light. Interference fringes can be observed near monochromatic caustics. A curved surface, like a lens, focuses light on some points and scatters it in others. The media that ensure the creation of such an effect are glass and water, which generates caustic waves.

Reflection, refraction and scattering of light when interacting with surfaces is difficult to calculate. Modelling the passage of light requires large computational costs. Visualization of dynamic scenes with changing lighting, materials, geometry, caustics and other three-dimensional effects in interactive mode is a big problem[1]. Generating caustics is a computationally expensive process, because it requires the simulation of many rays of light.

Monte Carlo methods are used for global illumination[2-4]. The papers [5] to [7] presents an overview of Monte Carlo methods for calculating light transfer in three-dimensional scenes. These methods are used to calculate physically correct scenes, but not at interactive speed. The articles [8–10] present a hybrid photon mapping method for global illumination. The density of photon maps is reduced due to selective photon storage. In places with high photon density, the radiation intensity is pre-calculated to speed up calculations. In [11–14], a method for calculating global illumination in real time for dynamic light scenes is presented[15-17]. The method is implemented based on approximate indirect lighting. Form factors are calculated for each surface during the preliminary operation. Only the largest ones are saved for rendering. Indirect illumination with a single reflection is calculated with a stored large coefficient as light sources. Indirect illumination with multiple reflections is approximated by the average intensity of reflection. The accuracy of a single indirect illumination is increased by using a brightness compensation algorithm[18-21].

The calculation of direct illumination from a polygonal light source, consisting of the integral of the triple product of illumination, the distribution function of bidirectional reflection (BRDF) and the visibility function is given in [22– 24].

*rom8591@gmail.com

Photonics Applications in Astronomy, Communications, Industry, and High Energy Physics Experiments 2022, edited by Ryszard S. Romaniuk, Andrzej Smolarz, Waldemar Wójcik, Proc. of SPIE Vol. 12476, 124760Y
© 2022 SPIE · 0277-786X · doi: 10.1117/12.2659704

In [25-27], a calculation of the ratio of the direct illumination equation is proposed, which allows combining analytical lighting methods with stochastic shadows tracked by rays, while maintaining correctness. It is shown that shaded lighting can be divided into the product of unshaded lighting and shadow weighted by illumination. However, these methods are not very well suited for visualizing caustics, since the high-frequency light transfer that forms caustics must be represented in the corresponding basic functions. In [28], an approach is proposed that allows interactively displaying caustics. A volume-tracing algorithm capable of creating multiple refractions is presented.

The paper [29] presents a method for visualizing single scattering in large scenes with reflecting and refractive objects and homogeneous media. Efficiency is achieved by calculating the final radiation along the viewing beam directly from the illumination beams. If the beams pass near the view beam, you can quickly identify such lighting beams in the scene. With this approach, the results are similar to the volumetric mapping of photons.

Our paper presents a method for visualizing volumetric caustics in single-scattering media based on beam tracking. The scene is visualized from the point of view of the light source, to determine the place of the first interaction of light and patches of free forms. Then the ray tracking method is used to process two-way refraction and multiple reflections. The beam generation depends on the geometric inhomogeneities of the mirror objects and the light intensity in the case of point light sources. No preliminary calculations are required in the method. By using limiting volumes, the number of calculations is reduced. The method supports multiple reflections of light and adaptively generates rays for visualization of caustics.

The main purpose of the proposed work is to develop a method of interactive visualization of caustics, in which it is necessary to separate the distribution of caustic photons, starting from light sources, from the collection of photons scattered in the direction of the camera. The collection of scattered light is performed during rasterization, which solves the problem of line of sight. The accumulation of light contribution using limiting volumes is largely associated with rasterization costs. A combination of the caustic mapping approach with caustic rendering is used. This ensures adaptive sampling in the image space of light while minimizing rasterization costs.

2. DESCRIPTION OF THE METHOD

2.1 Patches of free forms

Four planes, p1, p2, p3, p4, define the base triangle, p5 are normal vectors (Fig. 1).

1. (point – v2, p1) > 0
2. (point – v2, p2) > 0 (1)
3. (point – v3, p3) > 0
4. (point – v2, p4) > 0

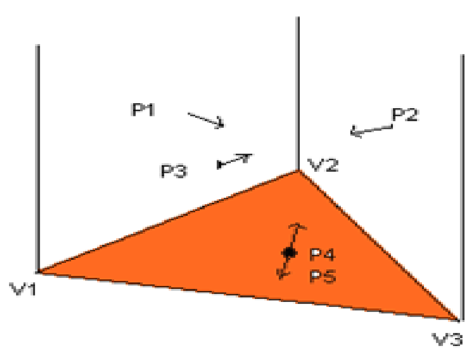

Figure 1. The base triangle.

A free-form patch is a composition of a basic triangle and a perturbation[18]:

$$F^{'}(x,y,z) = F(x,y,z) + \sum_{i=1}^{N} R_i(x,y,z) \quad (2)$$

where R(x,y,z) is a perturbation. The perturbation function R(x,y,z) is as follows:

$$R_i(x,y,z) = \begin{cases} Q_i^3(x,y,z), \ if \ Q_i(x,y,z) \geq 0 \\ 0, \ if \ Q_i(x,y,z) < 0 \end{cases} \quad (3)$$

where Q(x,y,z) is a perturbing quadric.

Figure 2 shows a free-form patch.

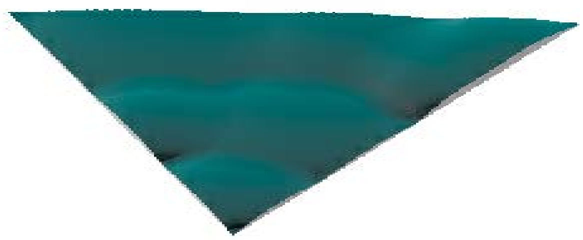

Figure 2. Free-form patch.

2.2 Main steps of the method

1. Generation of perturbation functions of patches of free forms.
2. All visible surfaces from the light source are rasterised, which are stored in the light buffer (Fig. 3).
3. The grid 64×64 is projected onto the scene.
4. Rasterization of the limiting volumes of caustic rays. For rays, the radiation scattered in the direction of the camera is calculated, depending on the phase function and the density of the medium.

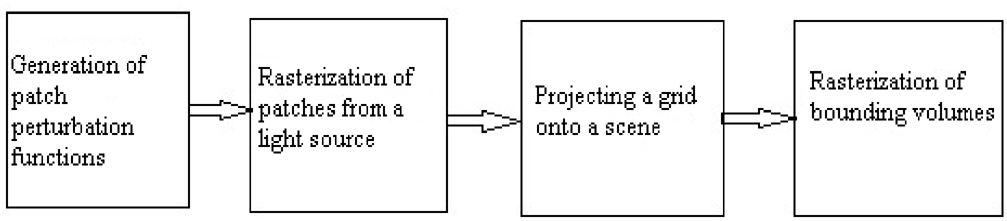

Figure 3. General scheme of the method.

Let's describe these steps in more detail. In the first step, the mirror surfaces visible from the light source are rasterized. The light buffer stores coordinates, normals and material properties, i.e. transparency, refractive index, etc. This ensures two-dimensional parameterisation of illuminated surfaces. Texture parameterisation is used to project a flat mesh onto illuminated surfaces. If you use a mesh with texture parameterisation, the projection step is simplified. Since the vertices can be moved to positions selected from the corresponding positions of the light buffer. The projected grid is a reduced, piecewise linear approximation of illuminated surfaces. The advantage of this method is the separation of geometric complexity from the caustic generation process. The grid has a resolution 64×64, the grid areas may not match the caustic sample. The grid cells are treated as two triangles. The bases of triangles with clipping planes form bounding volumes (Fig. 1).

The projection grid is used to create caustic rays that adapt to the inhomogeneities of the mirror object. The rays are also adapted to the characteristics of light emission and the contribution of the rays to the final image. The grid and the light source determine the incident rays on the caustic surface. It depends on the irregularities of the mirror surface, the beam energy and the camera parameters. This process is implemented using a geometric shader. The geometric shader allows you to output a variable number of vertices and generate data transfer back to memory. Next, a pixel shader works for fragments that are affected by caustic rays. A caustic ray is generated for each base triangle. Surfaces can be both reflective and refractive, as well as with multiple reflection of rays. To calculate the limiting volumes, the required length of the prism is determined, which is formed by three clipping planes (Fig. 1). The maximum length is calculated by crossing the rays with a truncated viewing angle. Only the caustic rays are rasterized, which make the main contribution to the resulting image.

At the last step of the method, the fragment shader calculates the amount of radiation scattered towards the observer. For each fragment, the camera beam intersects with the prism (Fig. 1), and the contribution is determined:

$$R(\omega) = \int_{\Delta l} e^{-c_e(l_1+l_2)} c_s(\vec{x}) f_p(\omega \cdot \omega^{'}) R_{in}(\omega^{'}) dl \quad (4)$$

here$R(\omega)$ is a radiation scattered towards the observer, Δl is an interval of intersection of the camera beam and the prism, $c_e$is an extinction coefficient, $c_s(\vec{x})$ is a scattering coefficient at the point$(\vec{x})$, $f_p(\omega \cdot \omega^{'})$ is a phase function, $l_1 + l_2$is a length of the path of light from the caustic triangle to the camera. The approximate calculation of the integral looks like this:

$$R(\omega) \approx \Delta l e^{-c_e(l_1+l_2)} c_s f_p(\omega \cdot \omega^{'}) R_{in}(\omega^{'}). \quad (5)$$

For each fragment, the shader calculates the intersection of the caustic ray and the ray coming from the observer. In addition, it calculates the radiation of the sample beam and its scattered contribution in the direction of the camera.

After calculating the intersection of the caustic beam and the beam coming from the observer, the radiation scattered in the direction of the observer is calculated:

$$R_s(\Delta\omega, \Delta p) = \int_{\Delta p} \int_{\Delta\omega} R(\vec{x}, \omega) \cos\alpha \, d\omega dA, \quad (6)$$

where $(\vec{x})$ is a point of the surface, Δp is a caustic patch, α is an angle between the normal and ω.

3. RESULTS

Figure 4 shows a test scene of a glass vessel with caustics. Testing was performed on a computer with an Intel Core2 CPU E8400 3.0 GHz processor, and a GeForce GTX 470 GPU (Table 1). The images were rendered with 1024×768 pixel resolution. The method is implemented using Direct3D 11 and HLSL. The shader architecture of Model 4 is sufficient for the method. The scene of a glass vessel contains an environment receiving caustics from a translucent model.

The complex effect of multiple refraction is shown. The refracted caustic rays are refracted again on the surface of the water. Caustics under the water surface are difficult in terms of performance. Since practically no caustic rays overlap. Therefore, the filling rate is very high. Surface caustics are interpolated between adjacent volumes of caustics using adjacent patches of free forms of caustics. For each vertex of the patch, an area function is used, which is averaged over caustic rays. The method of volumetric illumination for volumetric caustics is applied. The final image consists of direct illumination of the surface, volumetric illumination with shadows, surface and volumetric caustics.

Figure 4. Glass vessel with caustics.

Table 1. Test Scene performance.

Geometric operations	Rasterization	Number of caustic beams	Number of frames per second
18.6 milliseconds	20.4 milliseconds	4800	18

4. CONCLUSIONS

The paper presents a method for visualizing volumetric and surface caustics in an interactive mode with multiple reflections and refractions. The method is based on free form patches with perturbation functions and a ray-tracing algorithm. The method is implemented on programmable graphics hardware. The method uses calculations of limiting volumes for the effective accumulation of the contribution of caustic rays. Ray tracking is used for multiple reflections. By using adjacency information, smooth transitions between beams are generated. Due to this, the quality of surface caustics is significantly improved.

REFERENCES

[1] Avrunin, O. G., Tymkovych, M. Y., Pavlov, S. V., Timchik, S. V., Kisała, P., et al., "Classification of CT-brain slices based on local histograms," Proc. SPIE 9816, (2015).

[2] Eymet, V., Poitou, D., Galtier, M., Mouna, E. H., Terree, G., Fournier, R., "Application to the validation of fast radiative transfer solvers embedded in combustion simulators," Journal of Quantitative Spectroscopy and Radiative Transfer 127, 57-68 (2013).

[3] Eymet, V., Poitou, D., Galtier, M., Hafi, M. E., Terre, G., Fournier, R., "Null-collision meshless Monte-Carlo—application to the validation of fast radiative transfer solvers embedded in combustion simulators," Journal of Quantitative Spectroscopy and Radiative Transfer 129, 145-157 (2013).

[4] Christensen, P. H., Jarosz, W., "The path to path-traced movies," Foundations and Trends in Computer Graphics and Vision 10(2), 103-175 (2016).

[5] Bitterli, B., Jarosz, W., "Beyond points and beams: Higherdimensional photon samples for volumetric light transport," ACM Transactions on Graphics, Proc. Siggraph' 17, 36(4), (2017).

[6] Ament, M., Bergmann, C., Weiskopf,D., "Refractive radiative transfer equation," ACM Transactions on Graphics 33(2), 1-22 (2014).

[7] Belcour, L., Balak, K., Soler, C., "A local frequency analysis of light scattering and absorption," ACM Transactions on Graphics 33(5), 1-17 (2014).

[8] Booth, T. E., "Unbiased Monte Carlo estimation of the reciprocal of an integral," Nuclear Science and Engineering 156(3), 403-407 (2007).

[9] Bitterli, B., Jakob, W., Novak J., Jarosz, W., "Reversible jump Metropolis light transport using inverse mappings," ACM Transactions on Graphics 37(1), (2017).

[10] Brown, F. B., Martin, W. R., "Direct sampling of Monte Carlo flight paths in media with continuously varying cross-sections," Proc.of ANS Mathematics & Computation Topical Meeting, 6-11 (2003).

[11] Novak, J., Georgiev, I., Hanika, J., Jarosz, W., "Monte Carlo Methods for Volumetric Light Transport Simulation," Computer Graphics Forum 37(2), 551-576 (2018).

[12] Barnat-Hunek, D., Omiotek, Z., Szafraniec, M., Dzierżak, R., "An integrated texture analysis and machine learning approach for durability assessment of lightweight cement composites with hydrophobic coatings modified by nanocellulose," Measurement 179, 1-20 (2021).

[13] Gupte, S., "Real-Time Photon Mapping on GPU," CMSC 635 Advanced Computer Graphics, (2011).

[14] Wu, X., Chai, X., Wang, Y., Zhang, L., "Form-factor sampling based real-time global illumination," Journal of Computer-Aided Design and Computer Graphics 23(6), 941-948 (2011).

[15] Okuno, H., Iwasaki, K., "Binary space partitioning visibility tree for polygonal and environment light rendering," The Visual Computer 37(3), (2021).

[16] Heitz, E., Hill, S., McGuire, M., "Combining analytic direct illumination and stochastic shadows," Conference: the ACM SIGGRAPH Symposium, (2018).

[17] Schreiber, M., Atanasov, A., Neumann, P., Bungartz, H.-J., "Rendering of Feature-Rich Dynamically Changing Volumetric Datasets on GPU," Procedia Computer Science 29, 648-658 (2014).

[18] Sun, X., Zhou, K., Lin, S., Guo, B., "Line Space Gathering for Single Scattering in Large Scenes," ACM Transactions on Graphics 29(4), (2010).

[19] Vyatkin, S., Romanyuk, A., Romanyuk, O., Nechyporuk, M., Chekhmestruk, R., Mykhaylov, P., "Optimized Finite Element Method using Free-Form Volume Patches for Deformation of Three-Dimensional Objects," 10th International Conference on Advanced Computer Information Technologies (ACIT-2020), 845-850 (2020).

[20] Zabolotna, N. I., Pavlov, S. V., Ushenko, A. G., Sobko, O. V., Savich, V. O., "Multivariate system of polarization tomography of biological crystals birefringence networks," Proc. SPIE 9166, (2014).
[21] Omiotek, Z., Kotyra, A., "Flame image processing and classification using a pre-trained VGG16 model in combustion diagnosis," Sensors 21(2), 1-15 (2021).
[22] Błaszczak, U., and Zając, A. S., "Selected metrology problems implied by the application of led technology in lighting,". Informatyka, Automatyka, Pomiary w Gospodarce i Ochronie Środowiska, 6(3), 6-11 (2016). https://doi.org/10.5604/20830157.1212257.
[23] Vassilenko, S., Teixeira, J. P., Pavlov, S., "Energy harvesting: an interesting topic for education programs in engineering specialities," Internet, Education, Science (IES-2016), 149-156 (2016).22Kvyetnyy, R., Bunyak, Y., Sofina, O., et al., "Blur recognition using second fundamental form of image surface," Proc. SPIE 9816, (2015).
[24] Kvyetnyy, R., Bunyak, Y., Sofina, O., et al., "Blur recognition using second fundamental form of image surface," Proc. SPIE 9816, (2015).
[25] Kvyetnyy, R. N., Romanyuk, O. N., Titarchuk, E. O., et al., "Usage of the hybrid encryption in a cloud instant messages exchange system," Proc. SPIE 10031, (2016).
[26] Olszewski, S., Komada, P., Smolarz, A., Lytvynenko, V., Savina, N., Voronenko, M., Vyshemyrska, S., Omelchuk, A., Lurie, I., "Some Features of the Numerical Deconvolution of Mixed Molecular Spectra," In: Lecture Notes in Computational Intelligence and Decision Making. ISDMCI 2019. Advances in Intelligent Systems and Computing 1020, 20-34 (2020).
[27] Vyatkin, S. I., Romanyuk, S. A., Pavlov, S. V., Wójcik, W., et al., "Using lights in a volume-oriented rendering," Proc. SPIE 10445, (2017).
[28] Romanyuk, O. N., Pavlov, S. V., Melnyk, O. V., Romanyuk, S. O., Smolarz, A., et al., "Method of anti-aliasing with the use of the new pixel model," Proc. SPIE 9816, (2015).
[29] Romanyuk, S. O., Pavlov, S. V., Melnyk, O. V., "New method to control color intensity for antialiasing," Control and Communications (SIBCON), 2015 International Siberian Conference 21-23 May (2015).